Available online at www.sciencedirect.com
SCIENCE DIRECT®
Journal of Process Control 16 (2006) 265–274
JOURNAL OF PROCESS CONTROL
www.elsevier.com/locate/jprocont

Model reduction and control of reactor–heat exchanger networks

Michael Baldea, Prodromos Daoutidis *

Department of Chemical Engineering and Materials Science, University of Minnesota, 421 Washington Ave. SE, Minneapolis, MN 55455, United States

Abstract

This paper focuses on the dynamics and control of process networks consisting of a reactor connected with an external heat exchanger through a large material recycle stream that acts as an energy carrier. Using singular perturbation arguments, we show that such networks exhibit a dynamic behavior featuring two time scales: a fast one, in which the energy balance variables evolve, and a slow time scale that captures the evolution of the terms in the material balance equations. We present a procedure for deriving reduced-order, non-stiff models for the fast and slow dynamics, and a framework for rational control system design that accounts for the time scale separation exhibited by the system dynamics. The theoretical developments are illustrated with an example and numerical simulation results.

Keywords: Model reduction; Nonlinear control; Energy recycle; Singular perturbations

1. Introduction

Integrated process networks, consisting of individual units interconnected through material and energy recycle, are the rule, rather than the exception in the process industries. The dynamics and control of such networks present distinct challenges, since, in addition to the nonlinear behavior of the individual units, the feedback interactions among these units, induced by the recycle, typically give rise to more complex overall network dynamics (e.g. [4,21,24,11]).

At the same time, the efficient transient operation of such networks can be of critical importance, as the current economic environment imposes frequent changes in operating conditions and objectives (e.g. changes in product grade and feed switching), requiring tighter coordination of the plant-wide optimization and advanced control levels [19]. A major bottleneck towards analyzing, optimizing and improving the control of process networks is the often overwhelming size and complexity of their dynamic models, which make dynamic simulation computationally intensive and the design of fully centralized nonlinear controllers on the basis of entire network models impractical (such controllers usually require extensive state information and are almost invariably difficult to tune, expensive to implement and maintain, and sensitive to measurement errors and noise). Indeed, the majority of studies on control of networks with material (e.g. [18,28]) and energy recycle (e.g. [25,5]) are within a multi-loop linear control framework. The strong coupling between the control loops in different process units in a process network has consequently been recognized as a major issue that must be addressed in a plant-wide control setting [23,17,22,9].

In our previous work [15,16], we considered networks and staged processes with high internal flows compared to the throughput. Within the framework of singular perturbations, we established that the large recycle induces a time scale separation, with the dynamics of individual processes evolving in a fast time scale with weak

* Corresponding author. Tel.: +1 612 625 8818; fax: +1 612 626 7246.
E-mail address: daoutidi@cems.umn.edu (P. Daoutidis).

0959-1524/$ - see front matter © 2005 Elsevier Ltd. All rights reserved.
doi:10.1016/j.jprocont.2005.06.007

interactions, and the dynamics of the overall system evolving in a slow time scale where these interactions become significant; this slow dynamics is usually nonlinear and of low order. Motivated by this, we proposed a method for deriving nonlinear low-order models of the slow dynamics, and a controller design framework comprising of properly coordinated controllers designed separately in the fast and slow time scales.

In [3], we focused on process networks with recycle, in which small quantities of inert components are present and a small purge stream is used for their removal. Adopting again a singular perturbation perspective, we established the presence of a slow dynamics associated with the inert, derived explicit descriptions of this dynamics and outlined a framework for rationally addressing the control of inert levels in the network.

In the present paper, we focus on the energetic aspects of process networks with high material recycle. We analyze a prototype system for which the large material recycle acts as an energy carrier. Specifically, we consider the case of a reactor where a highly exothermic set of reactions takes place, connected with an external heat exchanger through a large material recycle stream for more effective heat removal. Using singular perturbation arguments, we show that the dynamics of such networks typically exhibit two time scales, with the energy balance dynamics evolving in the fast time scale, and the material balance dynamics evolving in the slow time scale. We describe a method for deriving approximate, nonstiff, reduced-order models for the dynamics in each time scale that are suitable for analysis and control. Also, we propose a controller design framework that accounts for this time scale separation.

Throughout our derivations, we use the standard order of magnitude notation $\mathcal{O}(\cdot)$.

2. Dynamics of reactor–heat exchanger networks

In processes in which reactions with significant thermal effects are present, adiabatic reactor operation is not possible and direct heating/cooling for isothermal operation is often impractical or infeasible. In such cases, large material recycle streams are frequently used as heat carriers, connecting the reaction unit to an external heat exchange system [26]. This configuration allows for more efficient heat exchange, due to the high flowrates of the recycle and the heating/cooling medium. In addition, it affords the process designer a choice of heat transfer area that is independent of the geometry of the reactor itself. The efficiency of the external heat exchanger can be increased further by increasing the heat capacity of the recycle stream, either by using excess quantities of a reactant or by introducing an inert diluent in the recycle loop, along with a separation unit. Such configurations can be used in both batch and continuous processes, and are quite common in processes featuring fast, highly exothermic reactions (e.g. polymerization).

Existing literature on the control of reactor–external heat exchanger networks is relatively scarce, concerning mostly the implementation of linear [1,10] and nonlinear [6] control structures on specific processes. These studies report several control challenges, including difficult tuning of PID and model-based controllers due to the ill-conditioning of the process model.

In what follows, we show that the dynamics of process networks consisting of a reactor with an external heat exchanger typically exhibit two distinct time scales, and we derive reduced-order models for the dynamics in each time scale.

2.1. Modeling of reactor–external heat exchanger networks

We consider a process network, comprising of a reactor and a heat exchanger, as shown in Fig. 1. Let M denotes the reactor holdup, M_R the holdup in the tube side of the heat exchanger and M_c the holdup in the shell side. Let F_o be the feed flowrate to the reactor, F the effluent flowrate from the network, F_c the coolant flowrate and R the recycle flowrate. Let T_o be the temperature of the feed stream, T the reactor temperature, T_R the temperature of the reaction mass in the tube side of the heat exchanger, T_{co} and T_c the inlet and outlet temperature of the cooling medium, respectively. $\mathscr{C}$ components are present in the network and participate in $\mathscr{R}$ stoichiometrically independent reactions, with reaction rate r_i, $i = 1, \ldots, \mathscr{R}$ and stoichiometric matrix $\underline{\underline{S}} \in \mathbb{R}^{\mathscr{C} \times \mathscr{R}}$. We denote the heat of reaction vector by $\underline{\Delta H} = [\Delta H_1, \ldots, \Delta H_{\mathscr{R}}]^T$. We assume that the thermal effect of the reactions is very high and that the adiabatic operation of the reactor is not possible. In order to control the reactor temperature, the reaction mass is recycled at a high rate (compared to the feed) through the heat exchanger. For simplicity, we consider the density and heat capacity of the reactants and products (ρ and C_p) and of the cooling medium used in the heat exchan-

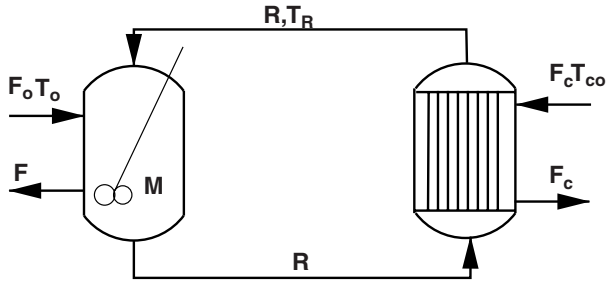

Fig. 1. Schematic diagram of a process network with external heat exchanger.

ger (ρ_c and C_{pc}) to be constant, and C_p and C_{pc} to be of comparable magnitude, i.e. $C_p/C_{pc} = k_{cp} = \mathcal{O}(1)$. Assuming that all units are modeled as lumped parameter systems and that the reactions only take place in the reactor, the model of the CSTR-external heat exchanger network becomes:

$$\begin{aligned}
\dot{M} &= F_o - F \\
\dot{\underline{C}} &= \underline{\underline{S}}\underline{r} + \frac{F_o}{M}(\underline{C_o} - \underline{C}) \\
\dot{T} &= -\frac{1}{C_p}\underline{\Delta H}^T\underline{r} + \frac{F_o}{M}(T_o - T) + \frac{R}{M}(T_R - T) \\
\dot{T}_R &= \frac{R}{M_R}(T - T_R) - \frac{UA}{C_p M_R}(T_R - T_c) \\
\dot{T}_c &= \frac{F_c}{M_c}(T_{co} - T_c) + \frac{UA}{C_{pc} M_c}(T_R - T_c)
\end{aligned} \tag{1}$$

where U denotes the overall heat transfer coefficient in the heat exchanger and A the heat transfer area.

Let us now define:

$$\varepsilon = \frac{F_{os}}{R_s} \tag{2}$$

where the subscript s denotes steady state values. Since the recycle flowrate R_s is much larger than the reactor feed F_{os}, $\varepsilon \ll 1$. Also, we define the scaled (potentially manipulated) inputs $u_o = F_o/F_{os}$, $u_F = F/F_s$, $u_R = R/R_s$ and $u_c = F_c/F_{cs}$, and the $\mathcal{O}(1)$ quantity $k_F = F_s/F_{os}$.

The model of Eq. (1) thus becomes:

$$\begin{aligned}
\dot{M} &= F_{os}(u_o - k_F u_f) \\
\dot{\underline{C}} &= \underline{\underline{S}}\underline{r} + \frac{F_{os}}{M}u_o(\underline{C_o} - \underline{C}) \\
\dot{T} &= -\frac{1}{C_p}\underline{\Delta H}^T\underline{r} + \frac{F_{os}}{M}u_o(T_o - T) + \frac{1}{\varepsilon}\frac{F_{os}}{M}u_R(T_R - T) \\
\dot{T}_R &= \frac{1}{\varepsilon}\frac{F_{os}}{M_R}u_R(T - T_R) - \frac{UA}{C_p M_R}(T_R - T_c) \\
\dot{T}_c &= \frac{F_{cs}}{M_c}u_c(T_{co} - T_c) + \frac{UA}{C_{pc} M_c}(T_R - T_c)
\end{aligned} \tag{3}$$

For useful energy removal, the rate of heat removal from the reactor by the recycle stream, $(RC_p(T - T_R))_s$, must be of the same magnitude as the rate of heat generation by the chemical reactions, $\Delta H_s = (-\underline{\Delta H}^T\underline{r}M)_s$:

$$k_{\Delta H} = \frac{\Delta H_s}{(RC_p(T - T_R))_s} = \mathcal{O}(1) \tag{4}$$

Equivalently,

$$\Delta H_s = \frac{1}{\varepsilon}k_{\Delta H}F_{os}C_p(T - T_R)_s \tag{5}$$

Our assumption (valid in most practical applications) that the heat capacities of the coolant and of the reaction mixture are of comparable magnitude, i.e.

$$\frac{C_p}{C_{pc}} = k_{cp} = \mathcal{O}(1) \tag{6}$$

implies that the flowrate of the external cooling utility stream in the heat exchanger will be in direct relationship with the reaction mass throughput, i.e. a high recycle rate will require a high coolant flowrate. Hence, we can assume that $F_{cs}/R_s = k_r = \mathcal{O}(1)$ and consequently $F_{os}/F_{cs} = \mathcal{O}(\varepsilon)$. At steady state, the cross-stream heat transfer rate in the heat exchanger and the net rate at which heat is input to the heat exchanger by the recycle stream R are identical:

$$\frac{(UA(T_R - T_c))_s}{(RC_p(T - T_R))_s} = 1$$

Additionally, we assume that the time constants for heat transfer and mass transport are of the same order of magnitude, i.e.

$$\frac{\frac{UA}{C_p M_R}}{\frac{R_s}{M_R}} = k_h = \mathcal{O}(1)$$

or, using Eq. (2),

$$\frac{UA}{C_p} = k_h\frac{F_{os}}{\varepsilon} \tag{7}$$

With the above notation, the dynamic model of the process network in Fig. 1 can be written as:

$$\begin{aligned}
\dot{M} &= F_{os}(u_o - k_F u_f) \\
\dot{\underline{C}} &= \underline{\underline{S}}\underline{r} + \frac{F_{os}}{M}u_o(\underline{C_o} - \underline{C}) \\
\dot{T} &= \frac{F_{os}}{M}u_o(T_o - T) + \frac{1}{\varepsilon}\frac{F_{os}}{M}u_R(T_R - T) \\
&\quad -\frac{1}{\varepsilon}\frac{k_{\Delta H}}{\Delta H_s}F_{os}(T - T_R)_s\underline{\Delta H}^T\underline{r} \\
\dot{T}_R &= \frac{1}{\varepsilon}\frac{F_{os}}{M_R}u_R(T - T_R) - \frac{1}{\varepsilon}\frac{k_h F_{os}}{M_R}(T_R - T_c) \\
\dot{T}_c &= \frac{1}{\varepsilon}\frac{k_r F_{os}}{M_c}u_c(T_{co} - T_c) + \frac{1}{\varepsilon}\frac{k_h k_{cp} F_{os}}{M_c}(T_R - T_c)
\end{aligned} \tag{8}$$

Due to the presence of flowrates of different magnitudes and of fast heat transfer, captured by the small singular perturbation parameter ε, the above model is stiff, its dynamics potentially featuring a two-time scale behavior. In the following section we document the two-time scale dynamics of the reactor–heat exchanger network, and obtain nonstiff, reduced-order models of the dynamics in each time scale.

2.2. Model reduction and control

We proceed with our analysis starting from the fast time scale. To this end, we define the "stretched", fast time scale $\tau = t/\varepsilon$ in which Eq. (8) becomes:

$$\begin{aligned}
\frac{dM}{d\tau} &= \varepsilon F_{os}(u_o - k_F u_f)\\
\frac{d\underline{C}}{d\tau} &= \varepsilon\left[\underline{\underline{S}}\underline{r} + \frac{F_{os}}{M}u_o(\underline{C}_o - \underline{C})\right]\\
\frac{dT}{d\tau} &= \varepsilon\frac{F_{os}}{M}u_o(T_o - T) + \frac{F_{os}}{M}u_R(T_R - T)\\
&\quad - \frac{k_{\Delta H}}{\Delta H_s}F_{os}(T - T_R)_s\underline{\Delta H}^T\underline{r}\\
\frac{T_R}{d\tau} &= \frac{F_{os}}{M_R}u_R(T - T_R) - \frac{k_h F_{os}}{M_R}(T_R - T_c)\\
\frac{T_c}{d\tau} &= \frac{k_r F_{os}}{M_c}u_c(T_{co} - T_c) + \frac{k_h k_{cp} F_{os}}{M_c}(T_R - T_c)
\end{aligned} \tag{9}$$

Then, we consider the limit $\varepsilon \to 0$, corresponding to infinitely large recycle and cooling medium flowrates and infinitely fast heat transfer in the heat exchanger. In this limit, we obtain the following description of the process network dynamics in the fast time scale:

$$\begin{aligned}
\frac{dT}{d\tau} &= \frac{F_{os}}{M}u_R(T_R - T) - \frac{k_{\Delta H}}{\Delta H_s}F_{os}(T - T_R)_s\underline{\Delta H}^T\underline{r}\\
\frac{T_R}{d\tau} &= \frac{F_{os}}{M_R}u_R(T - T_R) - \frac{k_h F_{os}}{M_R}(T_R - T_c)\\
\frac{T_c}{d\tau} &= \frac{k_r F_{os}}{M_c}u_c(T_{co} - T_c) + \frac{k_h k_{cp} F_{os}}{M_c}(T_R - T_c)
\end{aligned} \tag{10}$$

Notice that the large recycle and coolant flowrates u_R and u_C are the only manipulated inputs available in this fast time scale, and can be used to address temperature stabilization and regulation objectives.

In order to obtain a description of the slow dynamics, we first recognize that the equations describing the energy balance can be replaced, in the slow time scale, by the corresponding quasi-steady state constraints. These constraints are obtained by multiplying Eq. (8) by ε and considering the limit $\varepsilon \to 0$:

$$\begin{aligned}
0 &= \frac{F_{os}}{M}u_R(T_R - T) - \frac{k_{\Delta H}}{\Delta H_s}F_{os}(T - T_R)_s\underline{\Delta H}^T\underline{r}\\
0 &= \frac{F_{os}}{M_R}u_R(T - T_R) - \frac{k_h F_{os}}{M_R}(T_R - T_c)\\
0 &= \frac{k_r F_{os}}{M_c}u_c(T_{co} - T_c) + \frac{k_h k_{cp} F_{os}}{M_c}(T_R - T_c)
\end{aligned} \tag{11}$$

It is straightforward to verify that the algebraic constraints in Eq. (11) are generically linearly independent and hence they can be solved (analytically or numerically) for the quasi-steady state values $\underline{\Theta}^*(M, \underline{C}) = [T^*, T_R^*, T_c^*]$ of the variables $[T, T_R, T_c]$. Substituting the value for T^*, we then obtain:

$$\begin{aligned}
\dot{M} &= F_s(k_f u_o - u_F)\\
\underline{\dot{C}} &= \underline{\underline{S}}\underline{r}(T^*) + \frac{k_f F_s}{M}u_o(\underline{C}_o - \underline{C})
\end{aligned} \tag{12}$$

which represents the model of the slow dynamics of the reactor–external heat exchanger process network.

Note that only the small feed and effluent flowrates u_o and u_F are available as manipulated inputs in this slow time scale.

Remark 1. Due to the independence of the constraints (11), the system in Eq. (8) is in a standard singularly perturbed form [13], whereby one can distinguish between the fast variables $\underline{\Theta}$ (Eq. (10)), and the slow ones, M and $\underline{C}$ (Eq. (12)). Equivalently, the energy-related variables and the variables in the material balance of the reactor–heat exchanger network model evolve in different time scales, with the former being faster than the latter.

Remark 2. Fig. 2 illustrates the material and energy flows in the reactor–heat exchanger network. The rate of heat generation by the highly exothermic reactions, Q_{gen}, the rate of heat removal from the reactor by the large recycle stream acting as a energy carrier, $Q_{recycle}$, and the rate of heat removal from the network by the coolant, Q_{out}, are of comparable magnitude. These terms are much larger than the rate of heat removal by the reactor effluent (Q_F) and thus dominate the energy balance of the network.

On the other hand, the material throughput of the network is small, owing to the small reactor feed flowrate F. While the recycle rate R is much larger than the feed flowrate F, under the assumption that no reaction occurs outside the reactor, its composition remains constant. Therefore, the large recycle stream has no influence on the material balance of the network and the material balance equations do not contain any large terms. Based on these features, one can infer that the energy dynamics of the network, dominated by the large terms corresponding to the heat generation and removal through the heat exchanger, is faster than the dynamics of the material balance, which is characterized by the small material throughput. This conclusion is consistent with the results of the rigorous analysis presented above.

Remark 3. The material and energy balances of the network are not decoupled: notice that the rates of heat generation from the $\mathscr{R}$ reactions are the product of

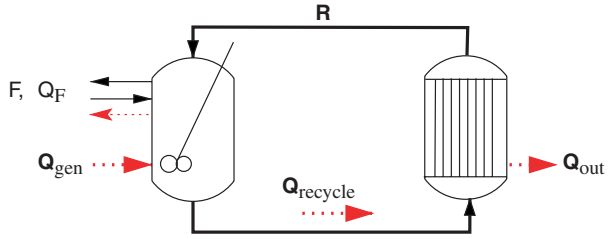

Fig. 2. Material (—) and energy (···) flows of different magnitudes in a reactor–external heat exchanger network.

two terms, ΔH_i and r_i, corresponding to the heat of reaction and reaction rate, respectively. Consequently, a high rate of heat generation by reaction could occur both in reacting systems in which fast reactions with moderate reaction enthalpies are present, and in reacting systems in which the reactions have moderate rates and a high heat of reaction. In the former case, the material balance of Eq. (12) will itself be in a nonstandard singularly perturbed form [27], and further reduction steps will be necessary in order to obtain nonstiff descriptions of the intermediate and slow dynamics. This issue is currently under investigation [2].

Remark 4. The analysis framework we presented is also applicable if an inert component is used to increase the heat capacity of the reaction mixture. In this case, the model (1) would be augmented by the equations corresponding to the model of the separation unit. However, the stoichiometric matrix $\underline{\underline{S}}$ and reaction rates $\underline{r}$ would remained unchanged, as the inert component does not partake in any reaction. Furthermore, the analysis can be applied if more complex correlations are used for the physical parameters of the system (e.g. temperature dependence of heat capacities and densities), as long as the basic assumptions (4), (6) and (7) are fulfilled.

Remark 5. The arguments presented above indicate that the control objectives related to the energy-balance related variables $\underline{\Theta}$ should be addressed using the large flows u_R and u_C, whereas the control objectives involving the slow variables in the material balance (such as the reactor holdup and product purity or distribution) should be addressed using the small flows u_o and u_F. Θ_{sp}, the setpoints of the controllers in the fast time scale are also available as manipulated inputs in the slow time scale, a choice that naturally leads to cascaded control configurations between the "energy" and "material balance" controllers.

Remark 6. In most cases, the only objective in the fast time scale is the control of the reactor temperature, for which there are two available manipulated inputs, u_R and u_C. Thus, several control system design options are available:

(i) control the reactor temperature using the coolant flowrate u_C as a manipulated input, while fixing R at its nominal value ($u_R = 1$),
(ii) use two controllers, one to control the reactor temperature using the recycle flowrate u_R, and the other to control the recycle stream temperature T_R with the coolant flowrate u_C,
(iii) use a single controller to control the reactor temperature and manipulate u_C and u_R, keeping the two flowrates in a fixed ratio. The ratio u_C/u_R depends on the cost of circulating the reaction mass and the cost of the coolant, and represents a design parameter.

Notice that in the first case the energy transfer between the reactor and the heat exchanger represents a bottleneck in the overall energy flow, which could lead to reactor runaway because of insufficient heat removal capacity. The second case overcomes this problem at the cost of a more elaborate control structure, while the third approach combines the benefits of the preceding two, i.e. it avoids the heat transfer limitations and relies on a simple control structure. In principle, (iii) can be regarded as using the net rate of heat removal from the reactor as a manipulated input for controlling the reactor temperature.

3. Simulation case study

Consider a process network such as the one in Fig. 1, with the parameters presented in Table 1. The feed stream of flowrate F_o contains the reactant A and its composition C_{Ao} is assumed to be constant. Two highly exothermic consecutive first-order reactions take place in the reactor:

Table 1
Nominal values for the process parameters (adapted from [20])

F	20 l/min
$F_{c,I} = R_I$	327.17 l/min
$F_{c,II} = R_{II}$	260.45 l/min
$F_{c,III} = R_{III}$	270.79 l/min
M	1200 l
M_R	22.93 l
M_c	68.8 l
C_{Ao}	2 mol/l
U	1987.5 $Wm^{-2} K^{-1}$
A	11.14 m^2
ΔH_1	−791.2 kJ/mol
ΔH_2	−527.5 kJ/mol
Ea_1	75.36 kJ/mol
Ea_2	150.72 kJ/mol
k_{10}	5.35×10^{10} min^{-1}
k_{20}	4.61×10^{18} min^{-1}
C_p	4138.2 J $l^{-1} K^{-1}$
C_{pc}	4138.2 J $l^{-1} K^{-1}$
T_o	311.1 K
T_{co}	294.4 K

	I	II	III
T, K	355.05	379.75	385.34
T_R, K	334.96	349.39	353.35
T_c, K	314.48	324.76	326.38
C_A, mol/l	7.43×10^{-2}	1.45×10^{-2}	1.031×10^{-2}
C_B, mol/l	1.891	1.323	0.995
C_C, mol/l	3.41×10^{-2}	0.662	0.995
Q_t, J/min	2.719×10^7	3.272×10^7	3.5839×10^7

Q_t represents the rate of heat transfer in the heat exchanger.

$$A \xrightarrow{k_1} B \xrightarrow{k_2} C \tag{13}$$

The purpose of the above process network is to produce either high purity B (containing as little C as possible), or a mixture of B and C with $C_B/C_C = 1$ or $C_B/C_C = 2$, at a given production rate. The objectives for this process are thus the control of the reactor temperature T, of the total holdup of the network (equivalent to the control of the reactor holdup M), and of the product purity C_B, at either operating points of interest.

Under the assumptions of Section 2.1, the model of the process network considered has the following form:

$$\begin{aligned}
\dot{M} &= F_0 - F \\
\dot{C}_A &= \frac{F_o}{M}(C_{Ao} - C_A) - k_{10}e^{-\frac{Ea_1}{RT}}C_A \\
\dot{C}_B &= -\frac{F_o}{M}C_B + k_{10}e^{-\frac{Ea_1}{RT}}C_A - k_{20}e^{-\frac{Ea_2}{RT}}C_B \\
\dot{C}_C &= -\frac{F_o}{M}C_C + k_{20}e^{-\frac{Ea_2}{RT}}C_B \\
\dot{T} &= \frac{F_o}{M}(T_o - T) + \frac{R}{M}(T_R - T) - \frac{\Delta H_1}{C_p}k_{10}e^{-\frac{Ea_1}{RT}}C_A \\
&\quad - \frac{\Delta H_2}{C_p}k_{20}e^{-\frac{Ea_2}{RT}}C_B \\
\dot{T}_R &= \frac{R}{M_R}(T - T_R) - \frac{UA}{C_pM_R}(T_R - T_c) \\
\dot{T}_c &= \frac{Fc}{M_c}(T_{co} - T_c) + \frac{UA}{C_{pc}M_c}(T_R - T_c)
\end{aligned} \tag{14}$$

which, by defining

$$\Delta H_s = \left(-\Delta H_1 k_{10}e^{-\frac{Ea_1}{RT}}C_A M - \Delta H_2 k_{20}e^{-\frac{Ea_2}{RT}}C_B M\right)_s$$

the small singular perturbation parameter

$$\varepsilon = \frac{F_{os}}{R_s}$$

the $\mathcal{O}(1)$ quantities

$$k_r = \frac{F_{cs}}{R_s}$$

$$k_f = \frac{F_s}{F_{os}}$$

$$k_{cp} = \frac{C_p}{C_{pc}}$$

$$k_{\Delta H} = \frac{\Delta H_s}{(RC_p(T - T_R))_s}$$

$$k_h = \frac{UA}{R_sC_p}$$

and the manipulated inputs $u_o = F_o/F_{os}$, $u_F = F/F_s$, $u_R = R/R_s$ and $u_c = F_c/F_{cs}$, can be rewritten as:

$$\begin{aligned}
\dot{M} &= F_{os}(u_o - k_f u_F) \\
\dot{C}_A &= \frac{F_{os}}{M}u_o(C_{Ao} - C_A) - k_{10}e^{-\frac{Ea_1}{RT}}C_A \\
\dot{C}_B &= -\frac{F_{os}}{M}u_oC_B + k_{10}e^{-\frac{Ea_1}{RT}}C_A - k_{20}e^{-\frac{Ea_2}{RT}}C_B \\
\dot{C}_C &= -\frac{F_{os}}{M}u_oC_C + k_{20}e^{-\frac{Ea_2}{RT}}C_B \\
\dot{T} &= \frac{F_{os}}{M}u_o(T_o - T) + \frac{1}{\varepsilon}\frac{F_{os}}{M}u_R(T_R - T) \\
&\quad - \frac{1}{\varepsilon}\frac{k_{\Delta H}}{\Delta H_s}F_{os}(T - T_R)_s \\
&\quad \times \left(\Delta H_1 k_{10}e^{-\frac{Ea_1}{RT}}C_A + \Delta H_2 k_{20}e^{-\frac{Ea_2}{RT}}C_B\right) \\
\dot{T}_R &= \frac{1}{\varepsilon}\frac{F_{os}}{M_R}u_R(T - T_R) - \frac{1}{\varepsilon}\frac{k_hF_{os}}{M_R}(T_R - T_c) \\
\dot{T}_c &= \frac{1}{\varepsilon}\frac{k_rF_{os}}{M_c}u_c(T_{co} - T_c) + \frac{1}{\varepsilon}\frac{k_hk_{cp}F_{os}}{M_c}(T_R - T_c)
\end{aligned} \tag{15}$$

We now apply the model reduction framework outlined in Section 2.2. In order to obtain a description of the fast dynamics, we define the fast time scale $\tau = t/\varepsilon$, and, in the limit of the recycle and coolant flow rate and the heat transfer coefficient in the heat exchanger becoming infinite i.e. $\varepsilon \to 0$, we obtain a description of the fast dynamics of the reactor–heat exchanger process network (15):

$$\begin{aligned}
\frac{dT}{d\tau} &= \frac{F_{os}}{M}u_R(T_R - T) - \frac{k_{\Delta H}}{\Delta H_s}F_{os}(T - T_R)_s \\
&\quad \times \left(\Delta H_1 k_{10}e^{-\frac{Ea_1}{RT}}C_A + \Delta H_2 k_{20}e^{-\frac{Ea_2}{RT}}C_B\right) \\
\frac{dT_R}{d\tau} &= \frac{F_{os}}{M_R}u_R(T - T_R) - \frac{k_hF_{os}}{M_R}(T_R - T_c) \\
\frac{dT_c}{d\tau} &= \frac{k_rF_{os}}{M_c}u_c(T_{co} - T_c) + \frac{k_hk_{cp}F_{os}}{M_c}(T_R - T_c)
\end{aligned} \tag{16}$$

According to the analysis in Section 2.2, we address the control of the reactor temperature T in the fast time scale, keeping the ratio u_C/u_R constant (Remark 6) and using the proportional–integral feedback law:

$$u_C = 1 + K_C\left(T - T_{sp} + \frac{1}{\tau_i}\int_0^t (T - T_{sp})\,dt\right) \tag{17}$$

The constraints arising from the fast dynamics (16) can now be solved for the quasi-steady state value, i.e. $T^* = T_{sp}$. Substituting T^* in Eq. (15), we obtain a description of the slow dynamics of the reactor–heat exchanger network:

$$\begin{aligned}
\dot{M} &= F_o - F \\
\dot{C}_A &= \frac{F_o}{M}(C_{A0} - C_A) - k_{10}e^{-\frac{Ea_1}{RT_{sp}}}C_A \\
\dot{C}_B &= -\frac{F_o}{M}C_B + k_{10}e^{-\frac{Ea_1}{RT_{sp}}}C_A - k_{20}e^{-\frac{Ea_2}{RT_{sp}}}C_B \\
\dot{C}_C &= -\frac{F_o}{M}C_C + k_{20}e^{-\frac{Ea_2}{RT_{sp}}}C_B
\end{aligned} \tag{18}$$

We consider that the flowrate of the feed stream F_o is fixed and, consequently, not available as a manipulated input in the slow time scale. Therefore, we address the control of the inventory of the network and of the product purity C_B by employing, respectively, F and T_{sp} as manipulated inputs, the latter choice leading to a cascaded control configuration.

Fig. 3 presents steady state profiles of concentrations as a function of temperature in the reactor. The temperature dependence of C_B exhibits a maximum at $T_{max} = 355.26$ K. However, operating the reactor at T_{max} is not feasible because $dC_B/dT|_{T=T_{max}} = 0$ (at $T = T_{max}$ controllability is lost) and the first requirement that calls for obtaining a product stream with a high concentration of B and a low concentration of C, is fulfilled by operating the reactor at $T_{sp,I} = 355.05$ K $< T_{max}$ (operating point I). On the other hand, the product mixture with $C_B/C_C = 2$ or $C_B/C_C = 1$ is obtained by operating the reactor at $T_{sp,II} = 379.75$ K $> T_{max}$ and, respectively, at $T_{sp,III} = 385.34$ K $> T_{max}$ (operating points II and III). Due to the different signs of the steady state gain of the process at operating point I, and at operating points II and III, any linear controller with integral action leads to instability if used *both* at operating point I and at operating points II and III, while a proportional controller leads to offset [7]. On the other hand, a nonlinear controller does not suffer from this limitation.

In what follows, we address the design of such a controller. We assume that switching between a product with $C_B/C_C = 2$ and a product with $C_B/C_C = 1$ is also required. Thus, in addition to good disturbance rejection abilities at all operating points, the controller is required to exhibit good setpoint tracking abilities between operating points II and III. Fig. 4 shows the

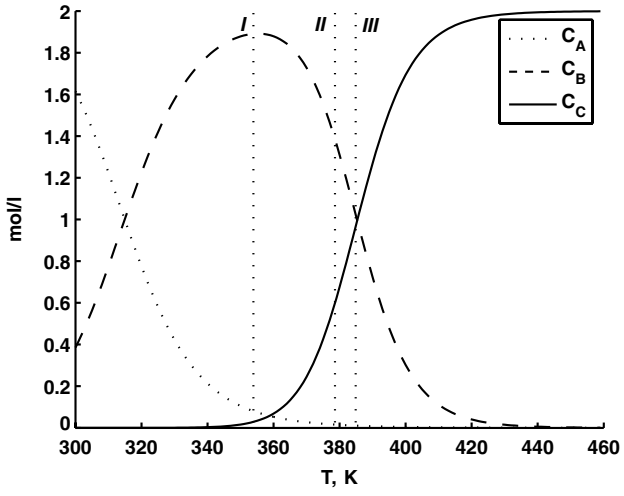

Fig. 3. Steady state reactor concentrations as a function of temperature.

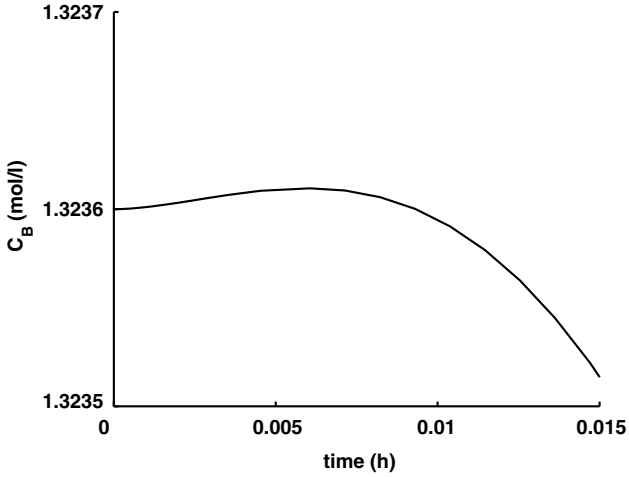

Fig. 4. Inverse response of the product purity C_B.

evolution of the product purity, initially at the steady state $C_B = 1.323$ mol/l, $T = 379.75$ K (operating point II) to a 1 K increase in T_{sp}. Notice that the product purity exhibits an inverse response. This nonminimum phase behavior originates in the increased contribution of the second reaction at temperatures higher than T_{max}. Namely, around operating point II, a rise in temperature leads to a rise in the rates of both the first and the second reaction. However, the rate of the first reaction is faster to increase than that of the second and, immediately after the temperature rise, more B is generated than consumed. Consequently, C_B increases. Subsequently, the consumption of B increases because the rate of the second reaction increases, and C_B falls as expected. A similar dynamic behavior is encountered around operating point III.

Motivated by the above, we address the design of the product purity controller for the reactor–external heat exchanger network by following the approach of statically equivalent outputs [12] in a manner analogous to [14]. To this end, we will construct an auxiliary output $\tilde{y}$ such that: (i) $\tilde{y}$ is statically equivalent to the process output C_B, i.e. $\tilde{y} = C_B$ at every steady state, and (ii) the system is minimum phase with respect to $\tilde{y}$ (and to the other output, M). Once such an output $\tilde{y}$ is constructed, an input/output linearizing controller will yield asymptotic tracking for C_B, with closed-loop stability. We consider a statically equivalent output (notice that this choice is not unique) of the form:

$$\tilde{y} = C_B + \gamma_{1,1}\frac{dC_B}{dt} + \beta\left[C_A + C_B + \gamma_{1,2}\frac{d}{dt}(C_A + C_B) - (C_{Ao} - C_C)\right] \quad (19)$$

with $\gamma_{1,1}$, $\gamma_{1,2}$ and β being scalar parameters. The above form is motivated by two factors:

- the term $C_B + \gamma_{1,1}\frac{dC_B}{dt}$ is statically equivalent to C_B, and corresponds to requesting a first order response in C_B when using a standard input–output linearizing controller. However, such a controller would lead to closed-loop instability, and the output requires a "statically equivalent" addition that would allow for overcoming this limitation,
- based on the arguments regarding the cause of the non-minimum phase behavior of the reactor–external heat exchanger network, the term

$$\beta\left[C_A + C_B + \gamma_{1,2}\frac{d}{dt}(C_A + C_B) - (C_{Ao} - C_C)\right]$$

is designed to cancel the influence of the second reaction on the concentration of A and B, by maintaining the sum $C_A + C_B$ at its "setpoint" $C_{Ao} - C_C$. Notice that $C_A + C_B + C_C = C_{Ao}$, and therefore the second term in Eq. (19) is zero at any steady state, that is, $\tilde{y}$ is statically equivalent to C_B.

With the outputs $\tilde{y}$ and M, based on the reduced-order model (18), a multivariable input–output linearizing controller with integral action [8] was designed for the product purity and reactor holdup, requesting a decoupled first-order response:

$$\tilde{y} = C_{B,sp} \tag{20}$$

$$M + \gamma_2\frac{dM}{dt} = M_{sp} \tag{21}$$

The controller was tuned with $\gamma_{1,1} = 30$ min, $\gamma_{1,2} = 57$ min, $\beta = 0.5$ and $\gamma_2 = 20$ min, and with the linear controller (17) tuned with $K_C = 0.15\ K^{-1}$ and $\tau_i = 2.8$ min, its performance was studied through simulations.

Initially, we considered the network at operating point I and tested the disturbance rejection abilities of the proposed control algorithm. We considered a −20% modeling error in the heat transfer coefficient U. Additionally, we assumed that at $t = 0$ an unmeasured 5.6 K rise occurs in the initial coolant temperature. The corresponding closed-loop behavior is presented in Figs. 5 and 6. The proposed control structure exhibits good performance, rapidly rejecting the disturbances by increasing the coolant flowrate. Notice also that the setpoint of the temperature controller T_{sp} exhibits very little variation in this case, as the modeling errors and disturbances considered act upon the temperature dynamics in the fast time scale and their effect on the slow time scale is very small. This observation is in complete agreement with the results of the theoretical analysis introduced in the first part of the paper.

Subsequently, we considered the network to be at operating point II ($C_{B,sp} = 1.323$ mol/l, corresponding to $C_B/C_C = 2$), and (at $t = 0$) we imposed a drop in the product purity setpoint to $C_{B,sp} = 0.995$ mol/l (operating point III, corresponding to $C_B/C_C = 1$). After 24 h of operation, the setpoint of C_B was raised to 1.323 mol/l, switching the operation of the network back to point II. Figs. 7 and 8 present the evolution of C_B, of the reactor temperature and of the coolant flowrate for this simulation. Observe that the proposed nonlinear controller exhibits good tracking performance between operating points II and III, as requested.

Finally, Figs. 9 and 10 show the closed-loop profiles for a 10% increase in the production rate at operating point I (attained by increasing F_o), and a decrease in the purity setpoint to $C_{B,sp} = 1.888$ mol/l—this reduction is necessary since the nominal purity is beyond the maximum attainable purity for the increased throughput. Note that, although controller design was carried out accounting for the inverse response exhibited

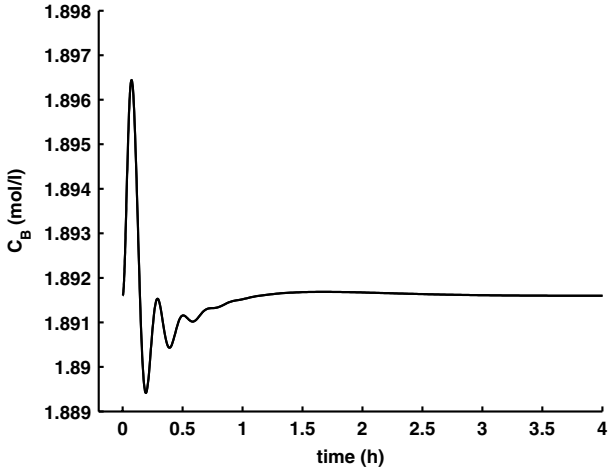

Fig. 5. Closed-loop evolution of the product purity in the presence of modeling errors and unmeasured disturbances.

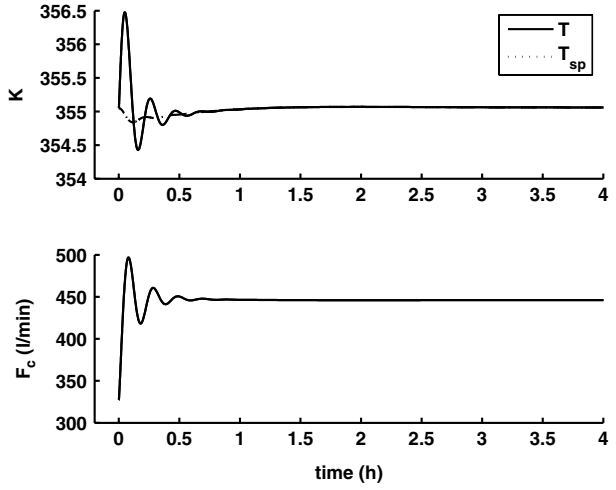

Fig. 6. Closed-loop evolution of the reactor temperature and of the coolant flowrate in the presence of modeling errors and unmeasured disturbances.

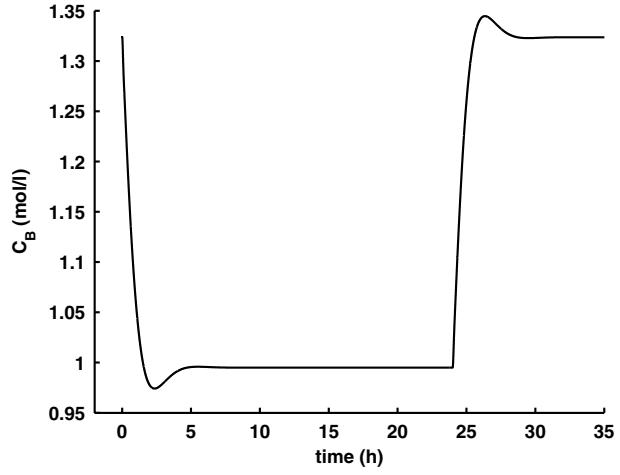

Fig. 7. Closed-loop profiles in the case of switching between operating points II and III.

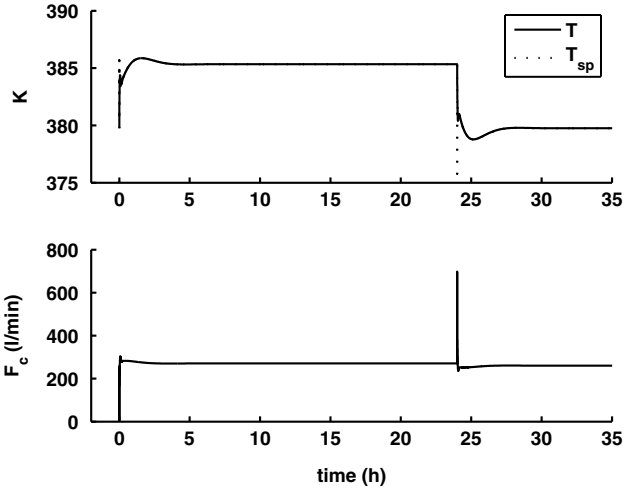

Fig. 8. Reactor temperature and coolant flowrate in the case of switching between operating points II and III.

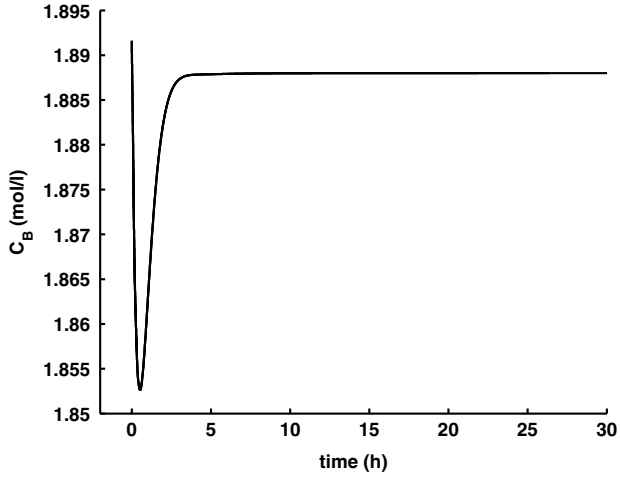

Fig. 9. Evolution of the product purity for a 10% rise in the production rate.

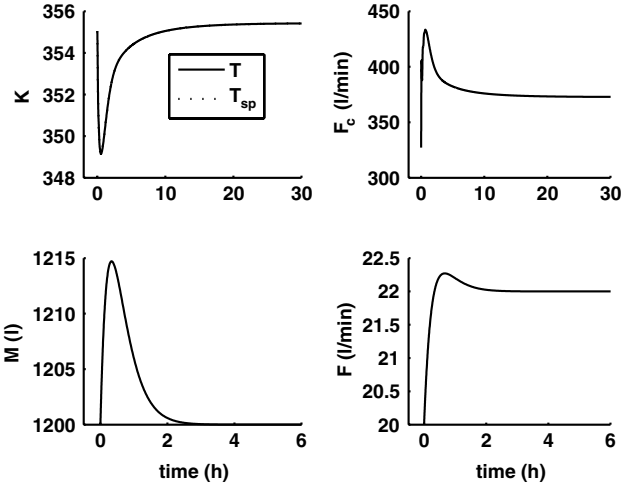

Fig. 10. Evolution of the reactor temperature, coolant flowrate, reactor holdup and effluent flowrate for a 10% rise in the production rate.

by the system at operating points II and III, the proposed control structure clearly yields good performance at operating point I as well.

4. Conclusions

In this paper, we analyzed the energy dynamics of a prototype process network with large recycle, specifically, a reactor with external heat exchanger. In this network, the large material recycle acts as an energy carrier. The presence of fast heat transfer and of material streams of largely different flowrates causes stiffness in the network model, its dynamics exhibiting a time-scale separation. Using singular perturbation arguments, we showed that the variables in the energy balance of these networks evolve in a fast time scale, while the terms in the material balance equations evolve in a slow time scale. Also within the framework of singular perturbations, we derived reduced-order, nonstiff models for the fast and slow dynamics of the network. Furthermore, our approach allowed for a rational separation of the available material flow rates into two distinct sets of manipulated inputs that act and can be used to address control objectives in the two time scales. Specifically, the large flowrates only act upon the fast dynamics, while the small ones act in the slow time scale. Finally, we provided an illustrative example for the proposed analysis and model reduction procedure, and presented numerical simulation results.

Acknowledgements

Partial support for this work by ACS–PRF, Grant 38114-AC9 and NSF–CTS, Grant 0234440 is gratefully acknowledged.

References

[1] E. Ali, K.L. Alhumaizi, Temperature control of ethylene to butene-1 dimerization reactor, Ind. Eng. Chem. Res. 39 (2000) 1320–1329.

[2] M. Baldea, P. Daoutidis, Dynamics and control of integrated process networks with multi-rate reactions, in: Proc. of the 16th IFAC World Congress, Prague, Czech Republic, in press.

[3] M. Baldea, P. Daoutidis, A. Kumar, Dynamics of process networks with recycle and purge: time scale separation and model decomposition, in: Preprints of ADCHEM'03, Hong Kong, 2004, pp. 645–650.

[4] C.S. Bildea, A.C. Dimian, Stability and multiplicity approach to the design of heat integrated PFR, AIChE J. 44 (12) (1998) 2703–2712.

[5] Y.H. Chen, C.C. Yu, Design and control of heat integrated reactors, Ind. Eng. Chem. Res. 42 (2003) 2791–2808.

[6] S.A. Dadebo, M.L. Bell, P.J. McLellan, K.B. McAuley, Temperature control of industrial gas phase polyethylene reactors, J. Proc. Contr. 7 (2) (1997) 83–95.

[7] P. Daoutidis, C. Kravaris, Dynamic output feedback control of minimum-phase nonlinear processes, Chem. Eng. Sci. 47 (1992) 837.

[8] P. Daoutidis, C. Kravaris, Dynamic output feedback control of minimum-phase multivariable nonlinear processes, Chem. Eng. Sci. 49 (1994) 433–447.

[9] C.A. Farschman, K.P. Viswanath, B.E. Ydstie, Process systems and inventory control, AIChE J. 44 (8) (1998) 1841–1857.

[10] L.S. Henderson, R.A. Cornejo, Temperature control of continuous, bulk styrene polymerization reactors and the influence of viscosity: An analytical study, Ind. Eng. Chem. Res. 28 (1989) 1644–1653.

[11] A.A. Kiss, C.S. Bildea, A.C. Dimian, P.D. Iedema, State multiplicity in CSTR-separator-recycle polymerization systems, Chem. Eng. Sci. 57 (2002) 535–546.

[12] C. Kravaris, M. Niemiec, R. Berber, C.B. Brosilow, Nonlinear model-based control of nonminimum-phase processes, in: R. Berber, C. Kravaris (Eds.), Nonlinear Model Based Process Control, Kluwer Academic Publishers, Dordrecht, 1998.

[13] A. Kumar, P. Daoutidis, Control of nonlinear differential equation systemsResearch Notes in Mathematics Series, vol. 397, Chapman & Hall/CRC, 1999.

[14] A. Kumar, P. Daoutidis, Modeling analysis and control of ethylene glycol reactive distillation column, AIChE J. 45 (1999) 51.

[15] A. Kumar, P. Daoutidis, Dynamics and control of process networks with recycle, J. Proc. Contr. 12 (2002) 475–484.

[16] A. Kumar, P. Daoutidis, Nonlinear model reduction and control for high-purity distillation columns, Ind. Eng. Chem. Res. 42 (2003) 4495–4505.

[17] M.L. Luyben, B.D. Tyreus, W.L. Luyben, Plantwide control design procedure, AIChE J. 43 (12) (1997) 3161–3174.

[18] W.L. Luyben, Dynamics and control of recycle systems. Parts 1–4, Ind. Eng. Chem. Res. 32 (1993) 466–486, 1142–1162.

[19] W. Marquardt, Fundamental modeling and model reduction for optimization based control of transient processes, in: Preprints of Chemical Process Control-6. Tucson, Arizona, 2000, pp. 30–60.

[20] G. Marroquin, W.L. Luyben, Practical control studies of batch reactors using realistic mathematical models, Chem. Eng. Sci. 28 (1973) 993–1003.

[21] J. Morud, S. Skogestad, Analysis of instability in an industrial ammonia reactor, AIChE J. 44 (1998) 888–895.

[22] C. Ng, G. Stephanopoulos, Plant-wide control structures and strategies, in: Proc. of DYCOPS-5. Corfu, Greece, 1998, pp. 1–16.

[23] R.M. Price, C. Georgakis, Plantwide regulatory control design procedure using a tiered framework, Ind. Eng. Chem. Res. 32 (1993) 2693.

[24] S. Pushpavanam, A. Kienle, Nonlinear behavior of an ideal reactor separator network with mass recycle, Chem. Eng. Sci. 57 (2001) 2837–2849.

[25] F. Reyes, W.L. Luyben, Steady-state and dynamic effects of design alternatives in heat-exchanger/furnace/reactor processes, Ind. Eng. Chem. Res. 39 (2000) 3335–3346.

[26] W.D. Seider, J.D. Seader, D.R. Lewin, Process Design Principles, John Wiley and Sons, Inc., New York, 1999.

[27] N.P. Vora, P. Daoutidis, Nonlinear model reduction of chemical reaction systems, AIChE J. 47 (2001) 2320–2332.

[28] C.K. Yi, W.L. Luyben, Design and control of coupled reactor/column systems—Parts 1–3, Comput. Chem. Eng. 21 (1) (1997) 25–68.